CONVERTING CHEMISTRY TO MINERALOGY FOR ACID AND METALLIFEROUS DRAINAGE RISK MANAGEMENT

J. Taylor[A], S. Winchester[B], M. Tyler[C], K. Ehrig[C], J. Waters[A] and F. Beavis[A].
[A]Earth Systems, 14 Church St., Hawthorn, VIC 3122, Australia
[B]GHD, 133 Castlereagh St., Sydney, NSW 2000, Australia
[C]BHP, 55 Grenfell St., Adelaide, SA 5000, Australia

ABSTRACT

Static geochemical data provides the foundation for quantifying the risk posed by sulfidic mine materials, including waste rock, tailings, wall rock, ore and low-grade ore stockpiles, heap leach pads and concentrate stockpiles. A new approach to developing a detailed acid and metalliferous drainage (AMD) risk layer for a mine model was recently developed for the Olympic Dam Fe-oxide Cu-U-Au-Ag deposit.

Major and trace element chemistry data from all resource drill holes are routinely collected at Olympic Dam. 65 analytical parameters, including carbon dioxide, were measured for a dataset of 10,000 samples, each representing a 15 m drill hole intersection. A program was developed to allocate the chemical components to 30 ore and gangue minerals known to occur at Olympic Dam, resulting in the production of a highly detailed modal mineralogy for each analysed intersection. The maximum potential acidity (MPA) and acid neutralising capacity (ANC) values were calculated from the key reactive minerals in each intersection. Key acidity generating minerals included pyrite, chalcopyrite, bornite and chalcocite. The dominant acid neutralising minerals included dolomite and ankerite; however, abundant siderite was also present. Net acid producing potential (NAPP) values were calculated from the MPA and ANC from each sample. AMD classification data identifying non-acid forming (NAF) and potentially acid forming (PAF) materials based on calculated NAPP values was produced for part of the deposit. 250 samples of drill hole material were collected and submitted to a NATA accredited laboratory for static geochemical analysis to assess the accuracy of the calculated mineralogy and associated NAPP values. The AMD risk classification for the laboratory data and the calculated mineralogy was shown to be well correlated.

It is concluded that bulk rock chemistry data can be used to accurately calculate mineralogy to develop AMD risk layers for mine block models, potentially dramatically improving AMD management and closure outcomes without the need for additional laboratory-generated geochemical data and at very little relative and absolute cost.

1.0 INTRODUCTION

The Olympic Dam mine is in South Australia, approximately 550 km northwest of Adelaide. The operation mines copper, uranium, gold and silver. While production commenced in 1988, the mine has been owned and operated by BHP Ltd (BHP) since 2005.

The copper mineralisation at Olympic Dam is associated with copper-bearing sulfides, including bornite (Cu_5FeS_4), chalcocite (Cu_2S) and chalcopyrite ($CuFeS_2$), together with pyrite (FeS_2), hosted in a hematite-rich breccia complex located beneath 350 m of unmineralised sedimentary rocks (BHP 2016). The ore body occurs to a depth of approximately 650 m in Precambrian basement rocks (BHP 2013). The basement rocks are overlain by a generally horizontally bedded overburden sequence comprising three main units. The deepest overburden unit is the Tregolana Shale, which immediately overlies the orebody. The Tregolana Shale is overlain by approximately 200 m of

Arcoona Quartzite, which is overlain by a 40-100 m thick deposit of the Andamooka Limestone (BHP 2013).

Operations at Olympic Dam comprise an underground mine, surface quarry, a mineral processing plant and associated infrastructure located within the Special Mining Lease (SML) area of approximately 180 km^2 (BHP 2016). The primary extraction method is a variant of sublevel open stoping, in which blocks of mineralised ore are systematically blasted and the ore recovered for crushing below ground. The crushed ore is then raised up one of the shafts to the surface stockpile (BHP 2016). Following extraction, stopes are backfilled with a cemented aggregate of crushed waste rock or crushed dolomite/limestone (BHP 2016). Above ground the metallurgical plant comprises a copper concentrator, a hydrometallurgical plant, uranium calciners, a copper smelter, a sulfuric acid plant, a copper refinery and a gold and silver refinery (BHP 2016).

1.1 Environmental Geochemistry

Previous studies (SRK 2008; AECOM 2010) have suggested that some Olympic Dam materials are potentially acid forming based on limited static geochemical data. These materials include granitic and hematitic major units and a minor laminated hematite-quartz sandstone/siltstone unit within the basement complex.

Future scenarios for Olympic Dam could include the construction of low grade ore (LGO) and waste stockpiles. These will contain elevated copper and sulfur concentrations. Dependent on the nature of these materials and future economic conditions, they may be stockpiled for 40 years or more. Approximately 60 million tonnes (t) of material may ultimately be stockpiled at Olympic Dam. The potential for acid formation in stockpiles and the occurrence of materials that may be used to manage PAF materials is largely unknown but important for the future.

1.2 Available Data

Between 2003 and 2008, BHP completed a routine assay program of approximately 1,000 surface diamond holes (~448,000 m) and approximately 1,600 underground diamond holes (Ehrig et al. 2012). Routine assays were conducted on composited samples over lengths of either 1, 2.5 or 5 metres. This equated to more than 1.3 million samples from the major and minor basement complex units analysed. These samples were analysed for Au, Ag, Al, As, Ba, Ca, Ce, Co, Cu, Fe, K, La, Mg, Mn, Mo, Na, Ni, P, Pb, S, Si, Ti, U_3O_8, Zn, Zr and CO_2. In addition, some 5,236 samples were assayed in overburden. The routine overburden assay included: Ag, Al, As, Ba, Bi, Ca, Cd, Ce, Co, Cr, Cu, Fe, K, La, Mg, Mn, Mo, Na, Ni, P, Pb, S, Sb, Si, Ti, U_3O_8, V, Y, Zn, Zr and CO_2.

Approximately 10,000 samples also underwent extended assaying (Ehrig et al. 2012). The samples were selected from the major and minor basement complex units and were collected on a widely spaced grid across the deposit. The extended assay involved analysing a composited sample over a sample length of between approximately 15 and 20 metres. The assay was for 65 elements including Ag, Al, As, Au, Ba, Be, Bi, Br, Ca, Cd, Ce, Cl, Co, Cr, Cs, Cu, Dy, Er, Eu, F, Fe, Ga, Gd, Hf, Ho, I, In, K, La, Li, Lu, Mg, Mn, Mo, Na, Nb, Nd, Ni, P, Pb, Pr, Rb, S, Sb, Sc, Se, Si, Sm, Sn, Sr, Ta, Tb, Te, Th, Ti, Tl, Tm, U_3O_8, V, W, Y, Yb, Zn, Zr and CO_2.

Mineralogy was also measured on the extended assay database using a Mineral Liberation Analyzer (MLA) (Ehrig et al. 2012). Quantitative XRD (X-ray diffraction) analysis was completed on 6,000 of the 10,000 samples. The MLA and XRD data generated a suite of up to 15 minerals per sample, but as no acid neutralising minerals were identified with these methods, the mineralogy could not be used to conduct acid-base accounting. The major mineralogy of the deposit was defined as quartz, hematite,

sericite, orthoclase, siderite, chlorite, barite, fluorite, chalcopyrite, albite, pyrite, bornite, rutile, ankerite, chalcocite, dolomite, crandallite and apatite (Ehrig et al. 2012). Minor and trace minerals include uraninite, coffinite, brannerite, florencite, bastnasite, cobalt sulphide, millerite, galena, sphalerite, molybdenite, zircon and carrolite (Reeve et al., 1990).

2.0 STUDY SCOPE

BHP engaged GHD Pty Ltd (GHD) and Earth Systems Consulting Pty Ltd (Earth Systems) to undertake a geochemical investigation of the Olympic Dam mineral waste and LGO to assess acid and metalliferous drainage (AMD) risk. Prior to this study, no comprehensive information on the static geochemistry of the ore, LGO and waste rock materials at Olympic Dam had been collected.

To generate an AMD Risk layer in the mine block model, two approaches were considered:

- Analyse thousands of (aged) existing samples for static geochemical parameters; or
- Use available bulk chemical data to calculate the mineralogy of the ore, LGO and waste rock materials, and use this information to calculate the net acid producing potential (NAPP) values of each sample.

The calculation approach was selected as the most appropriate and lowest cost method for obtaining new static geochemical data. This study describes the method for calculating the mineralogy and verifying the accuracy of using bulk chemistry data to classify the AMD risk of geologic materials.

3.0 METHOD

3.1 Calculation of Mineralogy

The method assumes a maximum of 31 minerals are potentially present in the basement rock types. These include primary and hydrothermal phases. Following careful examination of these minerals, a software tool was developed to assign elemental data and CO_2 from the extended assay bulk chemistry database to specific minerals in a sequence that minimised chemical ambiguity. For example, sulfur was initially stoichiometrically assigned to trace metals such as Zn, Pb, Co, Ni and Mo based on their occurrence as sulphide minerals (see below). Remaining sulfur was then stoichiometrically assigned to barite (as the only barium-bearing mineral). Any residual sulfur from this process was then assigned to the three copper sulphide minerals. All sulfur remaining after this process was assumed to be in the form of pyrite. The same method was applied to other silicate, carbonate and oxide phases. Following some experimentation, the optimum explicit order of element assignation was developed and is documented below.

Solid solution compositions for some minerals were varied to ensure that mineral percent totals were as close to 100% as possible. The order of assignment of elemental and CO_2 data to minerals is provided below. Specific solid solution compositions are also provided for each mineral phase.

- Uranium: Pitchblende / uraninite (UO_2), coffinite ($U(SiO_4)_{0.9}(OH)_{0.4}$), brannerite ($(U_{0.5}Ca_{0.3}Ce_{0.2})(Ti_{1.5}Fe_{0.5})O_6$);
- Cerium: Florencite ($CeAl_3(PO_4)_2(OH)_6$), bastnasite ($Ce(CO_3)F$);
- Zn, Pb, Co, Ni and Mo: Sphalerite (ZnS), galena (PbS), cobalt disulfide (CoS_2), millerite (NiS), molybdenite (MoS_2), carrollite ($CuCo_2S_4$);

- Barium: Barite ($BaSO_4$);
- Potassium: K-feldspar ($KAlSi_3O_8$), muscovite / sericite ($KAl_3Si_3O_{10}(OH)_2$), F-muscovite / F-sericite ($KAl_3Si_3O_{10}(OH)_{1.8}F_{0.2}$);
- Sodium: Na-feldspar ($NaAlSi_3O_8$), paragonite ($NaAl_3Si_3O_{10}(OH)_2$), F-paragonite ($NaAl_3Si_3O_{10}(OH)_{1.8}F_{0.2}$);
- Calcium: Dolomite ($CaMg(CO_3)_2$);
- Residual fluorine: Fluorite (CaF_2);
- Phosphorus: Hydroxyapatite ($Ca_5(PO_4)_3OH$), fluor-apatite ($Ca_5(PO_4)_3F$), apatite ($Ca_5(PO_4)_3OH_{0.33}F_{0.33}Cl_{0.33}$);
- CO_2 bearing phases: Siderite ($FeCO_3$), ankerite ($CaFe_{0.6}Mg_{0.3}Mn_{0.1}(CO_3)_2$);
- Titanium: Rutile (TiO_2), ilmenite ($FeTiO_3$);
- Residual Mg and Al: Chlorite ($Fe_3Mg_{1.5}AlFe_{0.5}(AlSi_3)O_{10}(OH,O)_8$), kaolinite ($Al_2Si_2O_5(OH)_4$);
- Copper and iron sulfide minerals: Chalcopyrite ($CuFeS_2$), bornite (Cu_5FeS_4), chalcocite (Cu_2S), pyrite (FeS_2);
- Zirconium: Zircon ($ZrSiO_4$); and
- Residual Fe and Si: Quartz (SiO_2), hematite (Fe_2O_3).

Algorithms for quantifying the relative proportion of different copper minerals were provided by BHPB staff. The assignation of sulfur to form sulfide minerals with Zn, Pb, Co, Ni and Mo was based on recorded mineralogy from the deposit (Reeve et al., 1990). Solid solution compositions were chosen based on available information for mineral chemistry, as well as by conducting controlled variations to minimise the deviation of mineral totals from 100%.

3.2 Calculation of AMD Risk

Once the modal mineralogy was calculated from the bulk chemistry data, the key acid forming and acid neutralising mineral phases were used to calculate a maximum potential acidity (MPA), an acid neutralising capacity (ANC) and thereby a NAPP value for each sample interval. The main acid generating phases were pyrite, chalcopyrite, bornite and chalcocite, while the key acid consuming phase was dominated by dolomite.

Siderite is both widespread and relatively abundant at Olympic Dam, but it has no net neutralising capacity. While it can initially neutralise acid, the eventual precipitation of ferrihydrite from the iron in siderite generates as much acid as it neutralises.

Earth Systems' AMDact software (Acid and Metalliferous Drainage assessment and classification tool), utilised the calculated MPA, ANC and NAPP values to produce an AMD risk classification for each sample interval. Positive NAPP values were nominated as potentially acid forming (PAF) and negative NAPP values were nominated as non-acid forming (NAF).

3.3 Verification Testing

To validate the accuracy of the AMD risk classification generated from the mineralogical calculations, a laboratory static geochemical testwork program was undertaken on a subset of 250 representative samples from the routine assay database.

Laboratory analysis included acid base accounting (ABA) (ANC and chromium reducible sulfur (S_{Cr})), and single addition net acid generation (NAG) testwork on all 250 samples. Acid buffering characteristics curves (ABCC) and total sulfur analyses were completed on a subset of 25 samples. Results were used to calculate the NAPP values for the 250 samples using S_{Cr} and ANC values. S_{Cr} data rather than total sulfur data was used to calculate NAPP values for the sample intervals due to the widespread occurrence of non-acid forming barite ($BaSO_4$) in the deposit. This approach minimised the inaccuracy of the laboratory data. The laboratory data was then processed using AMDact to quantify the AMD risk classification of each sample.

MPA, ANC, NAPP and AMD risk classifications that were calculated from modelled mineralogical data were compared with the laboratory data to assess the validity of the method.

4.0 **RESULTS**

The modal mineralogies of four of the 10,000 samples determined by strategic allocation of the extended elemental data and CO_2 to the mineral list provided above are shown in Table 1. Table 2 summarisies the AMD risk classifications based on the calculated mineralogy of the extended suite geochemical dataset for all 10,000 samples. The results indicate approximately 61% (n=6,115 of 10,002) of all samples were PAF, 99.6% (n=951 of 955) of ore samples were PAF, and some 92% (n=2,846 of 3,079) of all LGO samples were PAF. Approximately 61% (n=3,643 of 5,959) of waste rock samples were NAF, and 39% (n=2,316 of 5,959) PAF.

To verify the accuracy of the AMD risk classification generated from the mineralogical modelling, the laboratory derived acid-base accounting results were compared with the modelled data in Table 3. There is a relatively good correlation between the mean laboratory determined NAPP values and the mean calculated NAPP values for ore, LGO and waste rock. Median NAPP values were also comparable. The mean ANC also demonstrated a relatively good correlation for ore, LGO and waste rock between the two datasets.

Laboratory $NAG_{7.0}$ values were poorly correlated with laboratory NAPP (S_{Cr}) values, and poorly correlated with calculated NAPP values. The widespread occurence and relative abundance of siderite suggests that $NAG_{7.0}$ values may be under estimating the acidity generation associated with the oxidation of iron from siderite. This can happen in laboratory testwork if the NAG leachate undergoes titration prior to full oxidation of iron. The full oxidation and precipitation of iron generates acid, but this effect is not seen if the titration is conducted prematurely. This has the effect of erroneously assigning some neutralisation capacity to siderite. The disparity between $NAG_{7.0}$ values and NAPP (S_{Cr}) values suggests that the latter is more appropriate for comparison with calculated NAPP data.

Table 1. Example modal mineralogies for four samples

Mineral	Formula		1	2	3	4
Quartz	SiO_2	wt.%	54.5	36.2	16.9	7.79
K-Feldspar	$KAlSi_3O_8$	wt.%	14.6	1.68	0.28	0.03
Na-Feldspar	$NaAlSi_3O_8$	wt.%	0.00	0.27	0.21	0.15
Hematite	Fe_2O_3	wt.%	4.90	45.0	72.1	85.0
Muscovite / Sericite	$KAl_3Si_3O_{10}(OH)_2$	wt.%	0.00	0.00	0.00	0.00
F-Muscovite / F-Sericite	$KAl_3Si_3O_{10}(OH)_{1.8}F_{0.2}$	wt.%	21.6	3.62	0.61	0.06
Paragonite	$NaAl_3Si_3O_{10}(OH)_{1.8}F_{0.2}$	wt.%	0.00	0.27	0.20	0.00
Siderite	$FeCO_3$	wt.%	2.52	0.00	0.00	0.21

Mineral	Formula		1	2	3	4
Chlorite	$(Fe_3Mg_{1.5}AlFe_{0.5}(AlSi_3)O_{10}(OH,O)_8$	wt.%	0.00	1.35	0.87	0.00
Fluorite	CaF_2	wt.%	0.04	2.01	0.12	0.04
Barite	$BaSO_4$	wt.%	0.45	0.46	0.06	5.04
Ilmenite	$FeTiO_3$	wt.%	0.00	0.00	0.00	0.00
Kaolinite	$Al_2Si_2O_5(OH)_4$	wt.%	0.00	4.74	2.62	0.00
Dolomite	$CaMg(CO_3)_2$	wt.%	0.59	0.00	0.06	1.05
Pyrite	FeS_2	wt.%	0.00	2.16	3.07	0.26
Chalcopyrite	$CuFeS_2$	wt.%	0.38	0.00	2.63	0.13
Bornite	Cu_5FeS_4	wt.%	0.00	0.51	0.00	0.00
Chalcocite	Cu_2S	wt.%	0.00	1.21	0.00	0.00
Pitchblende / Uraninite	UO_2	wt.%	0.00	0.06	0.03	0.00
Coffinite	$U(SiO_4)_{0.9}(OH)_{0.4}$	wt.%	0.00	0.01	0.00	0.00
Brannerite	$(U_{0.5}Ca_{0.3}Ce_{0.2})\ (Ti_{1.5}Fe_{0.5})O_6$	wt.%	0.00	0.00	0.00	0.00
Florencite	$CeAl_3(PO_4)_2(OH)_6$	wt.%	0.03	0.12	0.07	0.06
Bastnasite	$Ce(CO_3)F$	wt.%	0.05	0.12	0.11	0.10
Cobalt Sulfide	CoS_2	wt.%	0.00	0.00	0.00	0.00
Millerite	NiS	wt.%	0.00	0.00	0.00	0.00
Galena	PbS	wt.%	0.00	0.01	0.00	0.00
Sphalerite	ZnS	wt.%	0.01	0.01	0.01	0.01
Molybdenite	MoS_2	wt.%	0.00	0.01	0.00	0.02
Rutile	TiO_2	wt.%	0.32	0.13	0.03	0.05
Zircon	$ZrSiO_4$	wt.%	0.06	0.02	0.01	0.00
Carrollite	$CuCo_2S_4$	wt.%	0.00	0.00	0.00	0.00
Total		wt.%	100.0	100.0	100.0	100.0

Table 2. AMD risk classification for 10,000 samples by material type

Material Type	General Classification		Detailed Classification					
	PAF	NAF	PAF				NAF	
			High Potential for Acid Generation (AG)	Moderate/High Potential for AG	Moderate Potential for AG	Low Potential for AG	Unlikely to be AG	Likely to be Acid Consuming
Waste	39%	61%	1%	5%	31%	2%	59%	2%
Ore	100%	0%	17%	55%	27%	1%	0%	0%
LGO	92%	8%	10%	39%	40%	3%	7%	1%

Table 3. Comparison of modelled and laboratory results by material type

Material type	pH (OX)	NAG (pH 4.5)	NAG (pH 7.0)	ANC		MPA (S_{CR})		NAPP (S_{CR})		Sulfur (S_{CR})	Sulfur
	pH Unit	kg H_2SO_4/t	kg H_2SO_4/t	kg H_2SO_4/t		kg H_2SO_4/t		kg H_2SO_4/t		wt.%	wt.%
	Laboratory	Laboratory	Laboratory	Laboratory	Modelled	Laboratory	Modelled	Laboratory	Modelled	Laboratory	BHP
LGO (n=150 samples)											
Maximum	9.10	25.8	50.4	100	247	95.5	98.4	87.0	97.3	3.12	3.76
Minimum	2.80	0.05	0.05	0.80	1.11	0.00	0.00	-92.7	-238	0.00	0.01
Mean	5.66	2.64	13.6	12.5	11.6	28.7	30.3	16.2	18.7	0.94	1.28
Median	5.30	0.05	9.65	8.80	3.89	21.6	23.0	10.2	13.2	0.71	1.06
Range	6.30	25.8	50.4	99.2	246	95.5	98.4	180	335	3.12	3.75
Ore (n=25 samples)											
Number samples	25	25	25	25	25	25	25	25	25	25	25
Maximum	8.80	11.4	60.0	112	100	138	135	120.5	126	4.51	4.97
Minimum	3.30	0.05	0.05	3.10	1.11	3.27	9.21	-87.7	-55.2	0.11	0.34
Mean	6.11	1.46	14.8	18.7	18.7	54.3	55.9	35.7	37.2	1.78	2.15
Median	6.40	0.05	1.60	9.00	8.22	49.6	47.6	36.0	32.8	1.62	2.16
Range	5.50	11.4	60.0	109	98.9	135	126	208	181	4.40	4.63
Waste (n=75 samples)											
Maximum	9.50	27.0	44.2	142	108	74.1	82.7	70.7	81.6	2.42	3.09
Minimum	2.80	0.05	0.05	1.80	0.69	0.18	0.00	-122	-107	0.01	0.01
Mean	6.79	0.67	3.61	19.1	13.0	9.12	10.4	-10.0	-2.57	0.30	0.69
Median	7.00	0.05	0.05	9.30	8.02	3.55	3.34	-5.11	-2.35	0.12	0.57
Range	6.70	27.0	44.2	140	108	73.9	82.7	193	188.7	2.41	3.08

5.0 DISCUSSION

While comparison of the statistics for NAPP (S_{Cr}) values and calculated NAPP values is encouraging, individual values are not always closely correlated. A key problem with this observation is that it is not clear which of the datasets is likely to be more accurate. The laboratory NAPP (S_{Cr}) values are based on the assumption that the key sulfide is pyrite, whereas the calculated NAPP values determine the specific sulfide species (pyrite, chalcopyrite, bornite, chalcocite, sphalerite, galena, cobalt disulfide, millerite, molybdenite and carrollite) and assign a modal mineralogy specific NAPP value. This suggests that the calculated NAPP values could be more accurate than the laboratory data.

Hence, to better assess the correlation between the two NAPP datasets, NAPP values were overlooked in preference to the AMD risk classification of each sample, a less sensitive but still fundamentally important metric. The correlation between NAF and PAF materials for ore, LGO and waste rock, as determined by laboratory testwork and mineralogical calcaulations, is displayed in Figure 1.

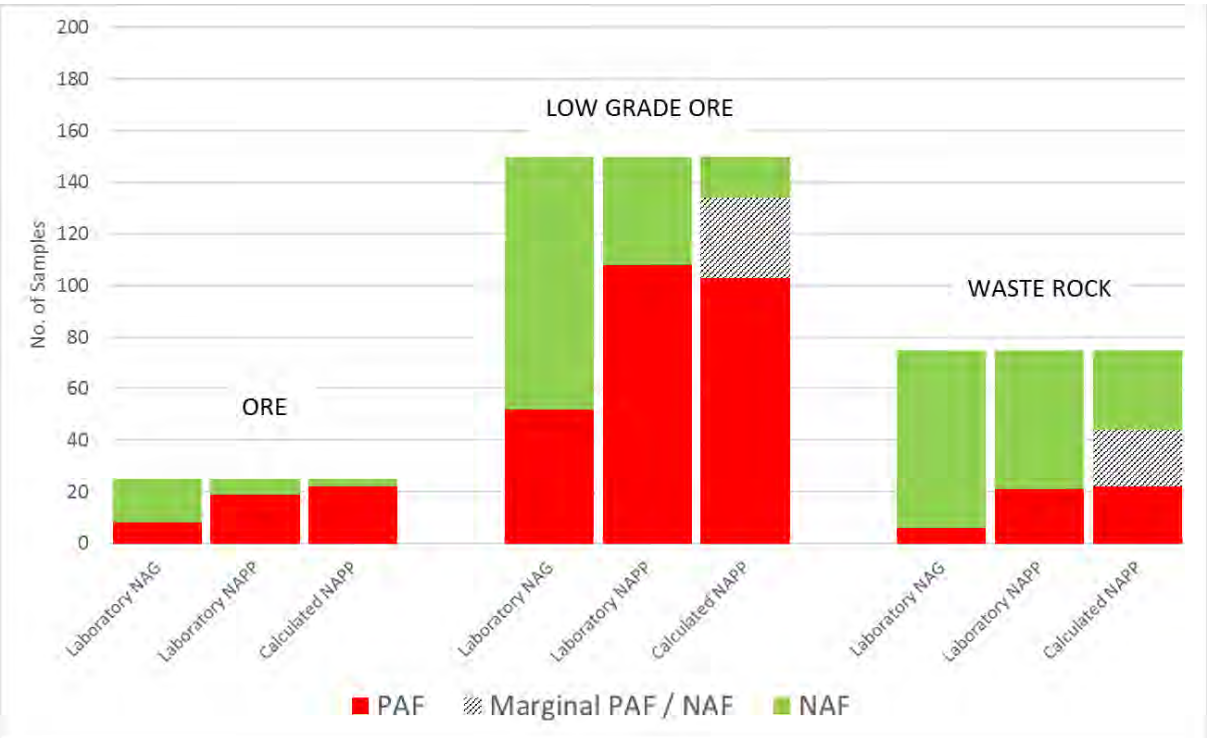

Figure 1. Comparison of AMD Risk classification between laboratory and calculated NAPP data

It is evident from Figure 1 that there is a very good correlation between AMD risk classification as determined for ore, LGO and waste rock materials, between laboratory NAPP (S_{Cr}) values and calculated NAPP values if we regard calculated NAPP values in the range -5 kg H_2SO_4/tonne to +5 kg H_2SO_4/tonne as effectively NAF (ie. marginal NAF/PAF). Figure 1 also highlights the poor correlation between laboratory $NAG_{7.0}$ values and either of the NAPP datasets.

6.0 CONCLUSIONS

The study has confirmed that it is possible to generate an AMD risk model for the Olympic Dam deposit using available bulk rock chemistry data to calculate detailed modal

mineralogical data, derive NAPP data and classify AMD risk, rather than conducting widespread and expensive re-analysis of geological samples. The study has also reinforced the importance of calculating the detailed mineralogical composition from major and trace components, rather than just establishing ANC from Ca, Mg and CO_2.

Classifying the AMD risk of the Olympic Dam deposit using the bulk chemistry database is key to understanding the AMD risk for operational and closure management at Olympic Dam. The integration of the AMD risk layer in the mine block model will facilitate short to long-term mine planning, ensuring that the LGO and waste rock is extracted and strategically placed to facilitate optimum metal recovery from LGO or effective AMD management.

It is concluded that bulk rock chemistry data can be used to accurately calculate mineralogy to develop AMD risk layers for mine block models, potentially dramatically improving AMD management and closure outcomes without the need for additional laboratory-generated geochemical data and at a low cost.

7.0 REFERENCES

AECOM (2010) Olympic Dam Kinetic Testing Program, Supplement to Appendix K5 of the Olympic Dam Draft EIS in BHP Billiton 2011, Olympic Dam Expansion Supplementary Environmental Impact Statement, Appendix F6.

BHP (2013) Olympic Dam Mine Closure and Rehabilitation Plan 2013. Document No. 99232 V3. September 2013.

BHP (2016) Olympic Dam Environment Management Manual. Document No. 2617 V20. 9 May 2016.

Ehrig K, McPhie J and Kamenetsky V (2012) Geology and Mineralogical Zonation of the Olympic Dam Iron Oxide Cu-U-Au-Ag Deposit, South Australia. *Society of Economic Geologists, Inc. Special Publication* 16: 237-267.

Reeve, J. S., Cross, K. C., Smith, R. N. and Oreskes, N., 1990. Olympic Dam Copper-Uranium-Gold-Silver Deposit, in Geology of the mineral deposits of Australia and Papua New Guinea (Ed. F. E. Hughes), pp. 1009-1035 (The Australian Institute of Mining and Metallurgy, Melbourne).

SRK (2008) Olympic Dam Expansion Assessment Olympic Dam Mine Rock Geochemistry in BHP Billiton 2009, Olympic Dam Expansion Draft Environmental Impact Statement, Appendix K5.